

discussions of their implications.

V. Experimental Section

The PMMA sample provided by Fudo Chemical Co. (Japan), with viscosity average molecular weight 10 000, is the same one used for solution measurements by one of us⁵ with a Twin-T a.c. bridge method to 150 MHz. The sample of PVAc, with weight average molecular weight 150 000, was made available to us by Professor W. J. McKnight (University of Massachusetts, Amherst). The sample of PMA, with number average molecular weight 63 200 and weight to number average molecular weight ratio 3.1, was obtained from Aldrich Chemical Co. Benzene and toluene were reagent grade. All compositions are expressed as weight percent.

Measurements of PMMA and PVAc in toluene were made at 23 ± 0.1 °C and of PMA in benzene at 6.6 ± 0.3 °C; both temperatures were maintained by a simple water bath surrounding the cell and adjusted coaxial line.

Numerical calculations from output data of the signal analyzer were made with the Brown University IBM 360/370 computer. The numerical Fourier transforms, based on eq 10, 11, or 12, were made with a Fortran program written by D. G. Hall.

VI. Discussion

The TDR methods we have described and illustrated have proved to be useful for measurements from 1 MHz to several GHz. Suitable choice of cell lengths in the basic design permits measurements of a wide range from strongly polar liquids to dilute solutions with small dispersion. In the latter case, it has been possible to define small relaxation processes, with maximum absorption ϵ_m'' of order 0.02, satisfactorily by use of the difference method

of comparison against pure solvent or other known reference liquid.

The methods used for time referencing, stabilization, and control have proved satisfactory and easy to use, but could probably be improved, as could some details of the cell construction to reduce minor effects, of small impedance mismatches for example. The performance realized, however, is in several respects close to limits imposed by the tunnel diode pulse generator and sampling oscilloscope.

The basic methods have been discussed primarily for liquids with negligible ohmic conductance, but their usefulness is not restricted to them. For appreciable specific conductance σ , the methods and working equations are still applicable as they stand with the proviso that the derived values of ϵ^* include the corresponding loss contribution. Thus a value $\epsilon_t^* = \epsilon^* + \sigma/i\omega\epsilon$ is obtained, where ϵ is the appropriate conversion factor for self-consistent units of ϵ^* and σ . Quite high specific conductances can be handled without undue loss in sensitivity as shown by recent results for H₂SO₄.¹⁰ In such cases modifications of the basic working equations to take explicit account of conductance σ are useful. These will be discussed elsewhere.

References and Notes

- (1) R. H. Cole, *J. Phys. Chem.*, **79**, 1459 (1975).
- (2) R. H. Cole, *J. Phys. Chem.*, **79**, 1469 (1975).
- (3) C. Shannan, *Proc. IRE*, **37**, 10 (1949).
- (4) H. A. Samulon, *Proc. IRE*, **39**, 175 (1951).
- (5) For definitions and discussion of this and the other relaxation functions, see C. J. F. Böttcher and P. Bordewijk, "Theory of Electric Polarization", Vol. II, Elsevier, New York, 1978.
- (6) S. Mashimo, A. Chiba, and K. Shinohara, *Polym. J.*, **6**, 170 (1974).
- (7) R. Iwasa and A. Chiba, *J. Polym. Sci., Polym. Phys. Ed.*, **15**, 881 (1977).
- (8) S. Mashimo and A. Chiba, *Polym. J.*, **5**, 41 (1973).
- (9) S. Mashimo and K. Shinohara, *J. Phys. Soc. Jpn.*, **34**, 1141 (1973).
- (10) D. G. Hall and R. H. Cole, *J. Chem. Phys.*, **68**, 3942 (1978).

Kinetics and Thermodynamics of Ion Pair Dissociation to Yield Free Solvated Ions. Effect of Steric Hindrance

Jeanette D. Kokosinski, Brad E. Forch, Gerald R. Stevenson,* Luis Echegoyen, and Carlos A. Castillo

Department of Chemistry, Illinois State University, Normal, Illinois 61761; and the Department of Chemistry, University of Puerto Rico, Río Piedras, Puerto Rico (Received December 3, 1979)

The kinetics and thermodynamics of ion pair dissociation involving the anion radicals of ninhydrin, nitrobenzene, and trialkyl-substituted nitrobenzenes ion associated with Na⁺, K⁺, Cs⁺, or (Bu)₄N⁺ in hexamethylphosphoramide (HMPA) were studied via ESR spectroscopy. The large alkyl groups on the (Bu)₄N⁺ cation were found to sterically inhibit the close approach of the positive nitrogen to the anion radical. However, this loose ion pair dissociates less exothermically and exoenergetically than tighter ion pairs involving the other cations due to the poorer solvation of this large cation by the HMPA. The alkyl groups in the ortho positions of the nitrobenzene anion radical also prevent close approach of a solvated cation to yield intimate ion pairs. These loose ion pairs have lower free energies of activation for ion pair dissociation. The observed rates and thermodynamics of ion pair dissociation and formation are explained in terms of ion solvation and steric inhibition to ion association.

Introduction

For a number of years it was generally thought that ion pair formation in solutions of ionophores (electrolytes which form ionic lattices in the solid state) was a consequence of electrostatic interactions exclusively. From these ideas the very useful equations of Bjerrum¹ and Fuoss² for estimating ion pair dissociation constants were derived. However, as we learned more about ion association it became apparent that there exists a number of exceptions

to the electrostatic models. The most notable solvent, which forms solutions of ionophores not obeying these models, is hexamethylphosphoramide (HMPA). HMPA has a relatively low dipole moment (4.48 D) and dielectric constant (29.6)³ but still dissolves many salts to form the unassociated solvated ions.⁴ The explanation of this lies in the fact that HMPA is one of the most powerful cation solvating agents known,⁵ and electrostatic theory is not able to predict the formation of such tightly solvated ions.⁶

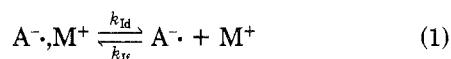
In agreement with this is the fact that the donor number for HMPA is very large (38.8).⁷ This, of course, rationalizes the deviation of HMPA solutions from electrostatic models but does not account for the qualitative or quantitative effect it has upon ion pair dissociation. Here, we report a systematic study of the thermodynamic and kinetic parameters controlling the ion pair dissociation for the ninhydrin anion radical-cation ion pairs and some symmetrical trialkyl-substituted nitrobenzene anion radical-potassium cation ion pairs coupled with some previously reported data to give a relatively complete picture of the ion association and ion-solvent interaction in this solvent. However, first it is necessary to indulge in some brief discussion of the nitrobenzene systems to be studied.

The fact that steric interactions between the ortho substituents on the nitro-aromatic compounds and the NO₂ group can result in twisting of the NO₂ group from the plane of the aromatic ring with consequent decoupling of the p orbitals involved has been recognized for almost 40 years.⁸ NMR, UV, and dipole moment studies of this effect in neutral nitro aromatics have been reviewed over 20 years ago.⁹ The effect was first observed upon the ESR spectra of anion radicals in 1961 when Geske and Ragle¹⁰ examined the ESR spectra of a series of methyl-substituted nitrobenzene anion radicals and observed a very large nitrogen hyperfine coupling constant of 17.8 G for the anion radical of 2,6-dimethylnitrobenzene in acetonitrile. For PhNO₂⁻ A_N is only 10.3 G in this solvent. The effect of the ortho substituent upon the spin densities far exceeds any mesomeric effect and is interpreted in terms of the twisting of the NO₂ group with consequent localization of the charge and spin densities on the nitro group.

Meisel and Neta^{11a} have noted that the one-electron reduction potential becomes more negative as the nitrogen coupling constant increases. In a recent report,^{11b} these same workers have shown that the rate constant for the transfer of an electron from (CH₃)₂COH to a nitro-aromatic neutral molecule decreases in a linear fashion with increasing A_N. This latter work was carried out in water where hydrogen bonding to the anion radical is an important factor in controlling its thermodynamic stability. However, their kinetic data reflect the lower stability of the twisted nitro-aromatic anion radicals despite their increased ability to act as a hydrogen bonding acceptors.

Hydrogen bonding and ion pairing are two of the most important solvation effects controlling the thermodynamic stability of anionic species in solution,¹² and for a variety of anion radicals the localization of charge density has been noted to stabilize the ion pair and hydrogen bonded species relative to the unassociated anion radical in hexamethylphosphoramide (HMPA) and in HMPA with added proton donors.^{13,14}

From the above, one might conclude that the degree of ion pairing of the anion radicals of 2,4,6-tri-*tert*-butylnitrobenzene and 2,4,6-triisopropylnitrobenzene in HMPA would be greater than in the anion radical of PhNO₂. This conclusion, however, is made without consideration of the possible steric inhibition to ion pair formation. In this report we discuss the free energies and free energies of activation for ion pair formation and dissociation involving the anion radicals of PhNO₂, *t*-Bu₃PhNO₂, and *i*-Pr₃PhNO₂ as well as the relative intimacy of the ion pairs among the different anion radicals.



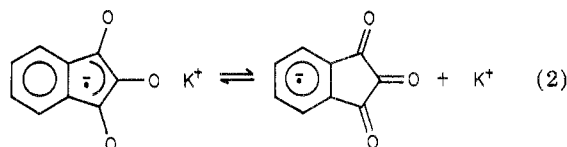
Since A^{·-}, M⁺ and A⁻ + M⁺ have different coupling constants and *g* values, these ESR parameters were used to monitor the free energy of eq 1. ESR relaxation times

were used to study the kinetics of this reaction. This information will lead to insight into the effect of steric interaction upon ion association thermodynamics and kinetics.

After the very first ESR investigations of ion pairing by Adam and Weissman¹⁵ and Atherton and Weissman,¹⁶ only a scattering of reports have appeared of actual rate constants of ion pair rearrangement to form solvent-separated ion pairs and just a single report of a rate constant for ion pair dissociation to form the free solvated ions.¹⁷ Rate constants for ion pair formation and dissociation are vital to the understanding of the mechanism of ion pair formation and dissociation. This report represents the first kinetic study of ion pair dissociation and formation for a variety of anions. Further, a new experimental technique is described for monitoring ESR line positions with a single-cavity EPR spectrometer.

Results and Discussion

The ninhydrin anion radical can be generated free of ion association in HMPA via the reduction of the neutral molecule in HMPA with sodium metal.¹⁸ The coupling constants for this solvated anion radical are 0.93 and 1.18 G.¹⁸ The addition of ionophoric perchlorates results in the formation of the ion pair between the anion radical and the added cation.¹⁹ This ion pair exists in rapid equilibrium with the unassociated ions, eq 2, and the ESR



spectrometer records only the time-averaged spectrum for the two species.¹⁹ Since the site of ion pair formation is the oxygen atoms on the ninhydrin anion, ion association results in the pulling of both spin and charge density away from the protons. This results in both proton coupling constants decreasing upon ion association.

It has been demonstrated that the weighted average total line widths ($\Delta\bar{w}_t$) vary to a greater extent than do the individual coupling constants upon ion association, and they can be used along with eq 2 for the determination of the ion pair dissociation constant:^{18,19}

$$1/(\Delta w_t^0 - \Delta\bar{w}_t) = K_{id}/[M^+](\Delta w_t^0 - \Delta w_t') + 1/(\Delta w_t^0 - \Delta w_t') \quad (3)$$

where $\Delta w_t'$ represents the spectral width for the ion pair, and Δw_t^0 represents that for the free ion.

Equation 3 has been utilized a number of times to determine ion pair dissociation constants,¹⁹⁻²¹ but there exists only a few examples of a measured enthalpy of dissociation for an ion pair that exists in rapid (on the ESR time scale) equilibrium with the free solvated ions.²² As it was our intention to determine the enthalpy and entropy changes for the reaction depicted in eq 3, it was necessary to generate plots of $1/(\Delta w_t^0 - \Delta w_t')$ vs. $1/[M^+]$ at several different temperatures for each of the cations to be studied. According to eq 2, these plots should be linear and have slopes of $K_{id}/(\Delta w_t^0 - \Delta w_t')$ and intercepts of $1/(\Delta w_t^0 - \Delta w_t')$. Such plots turned out to be linear (Figures 1 and 2), and the thermodynamic data taken from them and the respective van't Hoff plots are given in Table I. The same values for K_{eq} can be obtained by the use of weighted average *g* values.¹⁸

The addition of NaClO₄ to the ninhydrin anion radical solutions does not yield a change in the spectral parameters (*g* value or coupling constants) for the anion radical. Thus

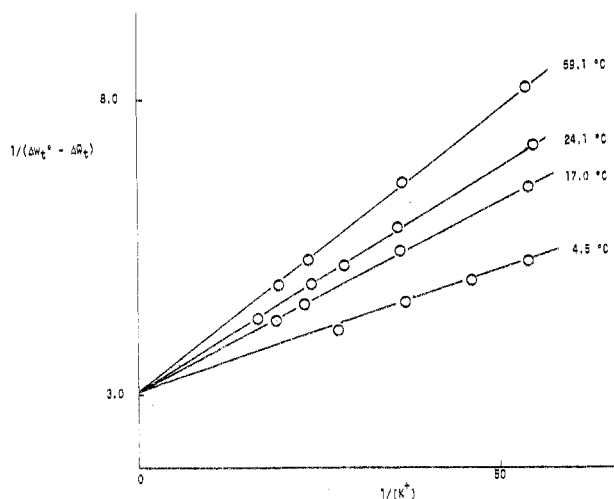


Figure 1. Plots of $1/(\Delta w_t^0 - \Delta w_t)$ vs. the reciprocal of the K^+ concentration in the HMPA solution of the ninhydrin anion radical at various temperatures.

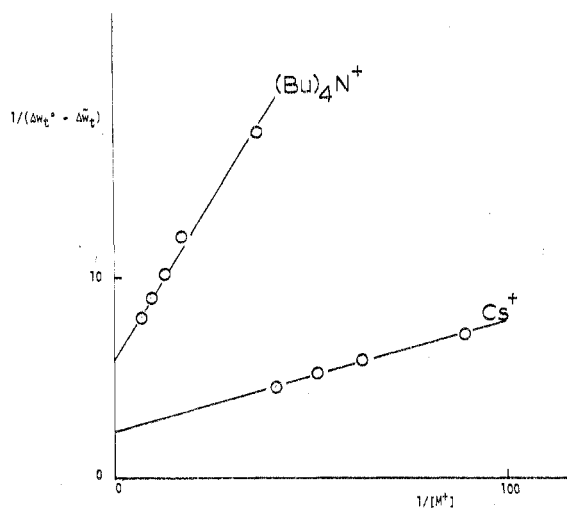


Figure 2. Plots of $1/(\Delta w_t^0 - \Delta w_t)$ vs. the reciprocal of the Cs^+ and $(Bu)_4N^+$ concentration in the HMPA solution of the ninhydrin anion radical.

TABLE I: Thermodynamic Parameters Controlling the Ion Pair Dissociation Depicted in Eq 2

M^+	K_{id} (25 °C)	ΔH° , kcal/mol	ΔS° , eu	$\Delta w_t'$
K^+	0.018 ± 0.002	-1.6 ± 0.1	-13.4	4.07
Cs^+	0.020 ± 0.004	-2.6 ± 0.1	-16.5	4.02
$(Bu)_4N^+$	0.052 ± 0.002	-0.12 ± 0.01	-5.9	4.20
Na^+	very large			

the K_{id} for the sodium ion pair dissociation must be larger than about 40. The lithium system also yields a very large value for K_{id} .

The equilibrium constants reported in Table I were reported earlier,¹⁹ but these are the first enthalpies of ion pair dissociation for these systems. The negative values for the entropy and enthalpy terms were expected and are due to the greater ordering of the solvent by the unassociated ions than by the ion pairs. Since the tetra-*n*-butylammonium ion is solvated by 6 to 7 HMPA molecules and the potassium cation by 4,¹⁹ it is surprising that this larger cation yields less negative entropy and enthalpy values. Evidently there is very little solvent reorganization upon the dissociation of this larger ion pair, and the cation and its solvation sheath must remain essentially intact upon ion pair formation. In contrast to this the potassium and cesium cations probably lose a solvent molecule in their solvation sheath upon ion pair formation. In support of this is the fact that $\Delta w'$ is smaller for the $(Bu)_4N^+$ ion

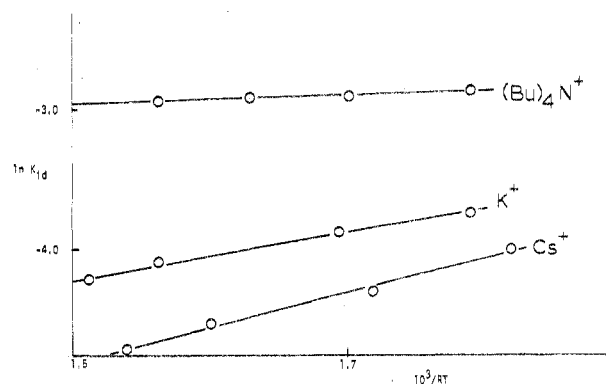


Figure 3. Van't Hoff plots for the ion pair dissociation of the ninhydrin anion radical in HMPA.

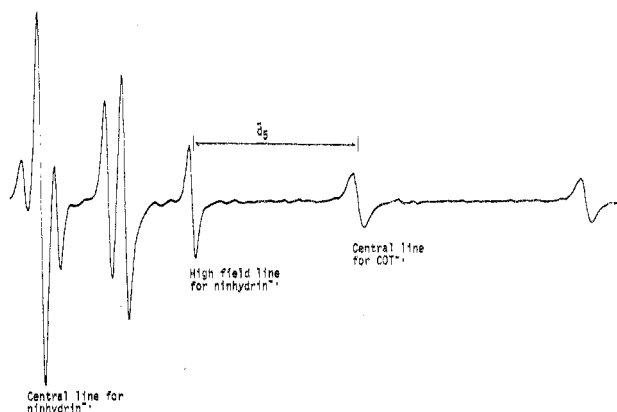


Figure 4. ESR spectrum of the ninhydrin anion radical in HMPA with 0.062 M added $KClO_4$. The spectrum is superimposed with that for the cyclooctatetraene anion radical also in HMPA. The cyclooctatetraene anion radical was contained in a capillary tube within the ESR tube containing the ninhydrin anion radical. Only the six high-field lines for the ninhydrin anion radical are shown. See Experimental Section.

pair, indicating that this cation causes a weaker perturbation upon the anion upon association with it.

The reorganization of the solvent sheath should sharply affect the rate constant for ion pair formation. It is expected that slower rate constants would be reflected from greater solvent reorganization. It turns out that the kinetic measurements are particularly convenient due to the large line width changes that take place upon ion pair formation (Figure 3).

Utilizing the measured coupling constants, g values, and K_{id} 's one can calculate the rate constant for the ion pair formation (k_{if}) and that for ion pair dissociation (k_{id}).¹⁷ This kinetic study is carried out by making use of the relaxation theory as applied to the two-site model, which has been derived in detail by Fraenkel.²⁰ His expression has been modified so that the kinetic parameters can be determined from the line heights, which change more rapidly than line widths with the lifetime of the spin state, eq 4. In eq 4 h_{-5} and h_5 are the heights of the low-field

$$\tau = \delta^0 \{ 1 - (h_5/h_{-5})^{1/2} \} 3^{1/2} |\gamma_e| / 2 \{ X_5 (h_5/h_{-5})^{1/2} - X_{-5} \} \quad (4)$$

and high-field lines, respectively, γ_e is the gyromagnetic ratio for an electron, δ^0 is the line width in the absence of ion pair formation, and X_m is related to the probability of finding the anion radical in the free state (P_f) or in the complexed state (P_c) as shown in eq 5, where $\omega_{f,m}$, $\omega_{c,m}$, and

$$X_m = P_f \{ \omega_{f,m} - \bar{\omega}_m \}^2 + P_c \{ \omega_{c,m} - \bar{\omega}_m \}^2 \quad (5)$$

$\bar{\omega}_m$ are the resonant frequencies of the m th line for the free ion, complexed ion, and the time-averaged species, respectively. These values can be easily measured from the

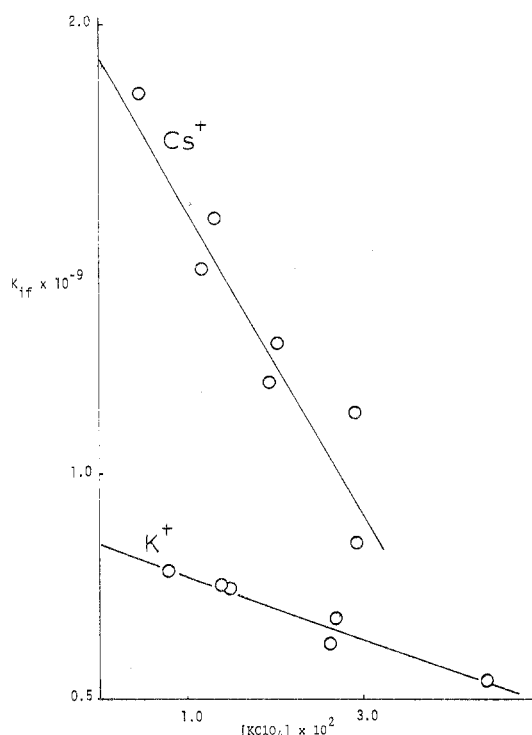


Figure 5. Plots of $k_{if,obsd}$ vs. the concentration of added $KClO_4$ or $CsClO_4$ for the ninhydrin anion radical in HMPA at 25 °C.

TABLE II: Dissociation Constants and Rate Constants for the Dissociation and Formation of Ion Pairs

ion pair	K_{id}	k_{id}, s^{-1}	$k_{if}, M^{-1} s^{-1}$
ninhydrin $^{\cdot-}$, K^+	0.018	1.5×10^8	$(8.4 \pm 0.2) \times 10^8$
ninhydrin $^{\cdot-}$, Cs^+	0.020	3.9×10^8	$(1.9 \pm 0.2) \times 10^9$
$PhNO_2^{\cdot-}$, K^+	10^{-3}	slow	
<i>i</i> -Pr $_3$ PhNO $_2^{\cdot-}$, K^+	1.5×10^{-3}	1.2×10^6	$(8 \pm 1) \times 10^8$
<i>t</i> -Bu $_3$ PhNO $_2^{\cdot-}$, K^+	3×10^{-3}	2.4×10^6	$(8 \pm 1) \times 10^8$

spectra taken with an internal standard as shown in Figure 4. τ is related to the lifetimes τ_f and τ_c of the free and complexed states as given by

$$\tau = \tau_f \tau_c / (\tau_f + \tau_c) \quad (6)$$

If we know the value for K_{id} , the rate constants can now be determined from τ , which is calculated from the experimental line heights and eq 4. The observed rate constants are related to K_{id} and τ as given by

$$K_{id} = \tau_f / \tau_c = k_{id} / k_{if} \quad (7)$$

$$k_{if} = \tau^{-1} (K_{id} + [M^+])^{-1} \quad (8)$$

From Figure 5, it is clear that the value for $k_{if,obsd}$ varies with the concentration of added salts. This is attributed to a number of factors including viscosity changes of the solution upon salt addition and changes in the activity coefficients of the ions. All of these problems are circumvented by an extrapolation of the observed rate constants to infinite dilution in added salt²¹ (Table II).

The expected result (k_{if} for the $K^+, N^{\cdot-}$ being larger than that for the $Cs^+, N^{\cdot-}$ ion pair) was not realized. In fact, substantially faster rates of ion pair formation and ion pair dissociation were observed for the less intimate $Cs^+, N^{\cdot-}$ ion pair. This must mean that the weaker interaction between the Cs^+ ion and the anion radical allows a more rapid exchange between anion radical and solvent molecule for the fifth coordination site around the Cs^+ ion in HMPA. This is consistent with the fact that the Cs^+ ion also forms weaker cation-solvent interactions in HMPA than does

TABLE III: Dissociation Constants, ESR Parameters, and Rates of Ion Pair Formation and Dissociation Relative to the ESR Time Scale for $PhNO_2^{\cdot-}$ Ion Pairs in HMPA at 25 °C

M^+	K_{id}	$A_N' - A_N^0$	rel rate
Na^+	0.15	2.4	slow
K^+	$< 10^{-3}$	1.5	slow
$(Bu)_4N^+$	4.8×10^{-4}	1.03	fast

K^+ cation.²³ Similar kinetic studies could not be carried out on the $(Bu)_4N^+$ system, because the rates of ion pair formation and dissociation were too fast.

Electrolytic reduction of nitrobenzene ($PhNO_2$) directly in the ESR cavity yields spectra in which both the ion pair and the free ion can be observed simultaneously. These spectra of $PhNO_2^{\cdot-}$ appear similar to those obtained via sodium reduction,^{13,24} but here the Na^+ concentration is known, allowing the determination of the ion pair formation constant. By comparing the ESR line intensities for the first lines of the ion pair and free ion and knowing the concentration of added Na^+ ions, one can determine $K_{id} = [Na^+][PhNO_2^{\cdot-}] / [PhNO_2^{\cdot-}Na^+]$ in the manner described for the semiquinone systems.²⁵ From solutions containing concentrations of Na^+ varying from 0.005 to 0.1 M, K_{id} was found to be 0.15 ± 0.04 . HMPA solutions of $PhNO_2^{\cdot-}$ containing even very low concentrations of KI or $KClO_4$ led to ESR spectra that were entirely due to the ion pair, and K_{id} for the $K^+, PhNO_2^{\cdot-}$ system was found to be too small to measure ($K_{id} < 0.001$). Since it has been demonstrated that the salts KI, $KClO_4$, and $NaClO_4$ are essentially fully dissociated in HMPA,²⁵ it was assumed that the cation concentration is equal to the total salt concentration.

When $(Bu)_4NClO_4$ was utilized as the electrolyte only the time-averaged species was observed. Thus, the rate of ion pair formation and dissociation is fast on the ESR time scale. The dissociation constant for $PhNO_2^{\cdot-}, (Bu)_4N^+$ can be obtained from the use of eq 9 if the two-site model

$$1/(\bar{A}_N - A_N^0) = K_{id} / [M^+] (A_N' - A_N^0) + 1 / (A_N' - A_N^0) \quad (9)$$

is correct,²⁶ where \bar{A}_N is the time-averaged nitrogen hyperfine coupling constant obtained from a solution containing a known quantity of $(Bu)_4NClO_4$, A_N^0 is this constant for the unassociated anion radical (8.48 G),²⁷ and A_N' is that for the ion pair. A plot of $1/(\bar{A}_N - A_N^0)$ vs. the reciprocal of the added $(Bu)_4NClO_4$ concentration is linear as predicted by eq 9 and yields a value of $(4.38 \pm 0.3) \times 10^{-4}$ and 1.03 for K_{id} and $A_N' - A_N^0$, respectively (Table III and Figure 4). This value for K_{id} would have been too small to measure had the rate of ion pair formation and dissociation been slow on the ESR time scale, as it is for the sodium and potassium systems.

Electrolytic reduction of either 2,4,6-tri-*tert*-butyl-nitrobenzene or 2,4,6-triisopropyl-nitrobenzene in HMPA with added KI yields the respective anion radical, which exhibits only a three-line pattern due to splitting from the ^{14}N nucleus.

Plots of $1/(\bar{A}_N - A_N^0)$ vs. $1/[K^+]$ are linear (Figure 6), and the dissociation constants are $(3.0 \pm 0.3) \times 10^{-3}$ and $(1.3 \pm 0.2) \times 10^{-2}$ for $t-Bu_3PhNO_2^{\cdot-}, K^+$ and $i-Pr_3PhNO_2^{\cdot-}, K^+$, respectively. Δg represents the difference in the observed g value for the anion radical with added KI and that for the free ion. Thus, a plot of $1/\Delta g$ vs. $1/[K^+]$ is also linear and has a slope of $K_{id}/\Delta g'$, where $\Delta g'$ is the difference in the g values for the free ion pair²⁸ (Figure 6).

The kinetic study was carried out by utilizing the same relaxation theory that was utilized for the ninhydrin sys-

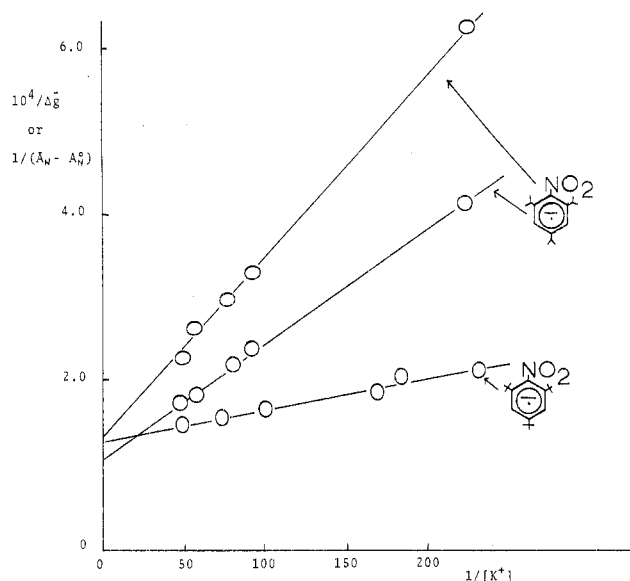


Figure 6. Plots of $1/(A_N^0 - \bar{A}_N)$ in G^{-1} vs. $[K^+]$ in M^{-1} for the anion radicals of 2,4,6-tri-*tert*-butylnitrobenzene and 2,4,6-triisopropylnitrobenzene and a plot of $10^4/\Delta g$ vs. $[K^+]^{-1}$ for the anion radical of 2,4,6-triisopropylnitrobenzene in HMPA at 25 °C. The g value and coupling constant plots yield the same values for K_{id} .

tems. The only difference is that eq 4 must be adopted to include the heights of the low-field and central lines of the nitro group triplet, h_{-1} and h_0 , respectively, eq 10.

$$\tau = \delta^0 \{ 1 - (h_{-1}/h_0)^{1/2} \} 3^{1/2} |\gamma_{el}| / 2 \{ X_{-1} (h_{-1}/h_0)^{-1/2} - X_0 \} \quad (10)$$

The rate constants were again taken from the intercept of a plot of $k_{if,obsd}$ vs. $[K^+]$ (Table II). The variation of $k_{if,obsd}$ for these systems is due to all of the factors that led to this variation in the ninhydrin systems plus the fact that unresolved proton hyperfine splitting may be present and varying with the concentration of added salt (degree of ion pairing). This problem is also nicely circumvented by an extrapolation of the observed rate constants to infinite dilution in KI (Table II).

Conclusions

From Table III it can be seen that the intimacy of the ion pairs involving $PhNO_2^-$ decreases as M^+ becomes larger, as evidenced by the larger $A_N' - A_N^0$ values or larger electronic perturbation upon the anion due to the smaller cations. Thus the tightly solvated Na^+ cation with its three closely associated HMPA molecules is hundreds of times less prone to form ion pairs than is K^+ , Cs^+ , or $(Bu)_4N^+$, but when the Na^+ ion pairs are formed they involve the most intimate association between cation and anion. The more intimate (tighter) ion pairing of the smaller cation is due to the fact that the Na^+ is coordinated by only three HMPA molecules¹⁹ and can approach the anion radical more closely than can the K^+ , Cs^+ , or $(Bu)_4N^+$. Further, since the smaller cations that form more intimate ion pairs are also better solvated on the right-hand side of eq 1, it is the ion pairs involving these cations that dissociate more readily. The positive nitrogen in the $(Bu)_4N^+$ ion is apparently prevented from coming into close proximity to the ninhydrin or $PhNO_2^-$ anion radical due to steric interactions involving the large butyl groups (Table I). The less intimate $(Bu)_4N^+$ ion pairs also dissociate with a less negative entropy change than do those involving the smaller cations. This is true, since the large $(Bu)_4N^+$ cation creates less ordering of the solvent on the right-hand side of eq 1.

Comparing the Cs^+ and K^+ ion pairs with the ninhydrin anion radical, the two parameters (ΔS° and ΔH°) cancel

each other yielding almost the same value for K_{id} . Both k_{id} and k_{if} are, however, significantly larger for the Cs^+ ion pair. In general, the larger ion pairs dissociate more rapidly than the smaller more intimate ones. The loose $PhNO_2^-$ ion pair involving the large poorly solvated $(Bu)_4N^+$ ion traverses a lower barrier to dissociation than do the smaller ion pairs.

From Table II one notes that both the rate of ion pair dissociation and K_{id} are increased by placing large alkyl groups in the ortho positions of the nitrobenzene anion radical. This is the case even though these groups increase the charge density at the site of ion pairing. This can only mean that the solvated K^+ ion is sterically prevented from close approach to the NO_2 group by the two isopropyl or *tert*-butyl groups. The fact that these ion pairs are less intimate than those of $PhNO_2^-$ is substantiated by the small $A_N' - A_N^0$ and $\Delta g'$ values. The energy barrier to dissociation is lower for the trialkyl $PhNO_2^-$ anion radicals, since the looser ion pairs involve less solvent reorganization upon dissociation.

Even though the *tert*-butyl group is larger than the isopropyl group, both K_{id} and k_{id} are larger for *i*- $Pr_3PhNO_2^-$ anion radical. However, the electronic perturbation caused by the association with K^+ ion is larger for the isopropyl system. This may be explained by the larger degree of distortion of the NO_2 group from planarity in the *tert*-butyl system than in the isopropyl system. In agreement with this is the fact that A_N^0 is larger for the *i*- $Pr_3PhNO_2^-$ anion radical.

For the dissociation of nitromesitylene anion radical ion pair with a series of cations in dimethylformamide (DMF) the dissociation constant was found to increase with the increasing size of the cation.²⁹ This trend of increasing ion association with decreasing cation size has been observed for the vast majority of solvent systems that have been studied.^{30,31} However, the reverse is the case in HMPA (Tables I and III). This trend in HMPA is explained in terms of the poorer solvation of the larger cations with the electronegative oxygen atom on the HMPA molecule.

It is instructive to compare the recent ion pair dissociation constants of Fawcett and co-workers²⁹ with those found by Toshima and Itaya³² for the nitrobenzene anion radical in DMF. At ambient temperature in DMF the ion pair dissociation constants between the nitromesitylene anion radical and Li^+ , Na^+ , and K^+ are 7.1×10^{-5} , 2.1×10^{-4} , and 1.5×10^{-3} , respectively.³⁰ When $PhNO_2^-$ serves as the anion, the constants are much larger, 2.9×10^{-3} , 4.5×10^{-3} , and 3.3×10^{-3} , respectively.³² This suggests that any steric hindrance tending to disrupt the ion pair due to the methyl groups on the nitromesitylene is more than offset by the increased charge density on the NO_2 group.

Steric interactions between the alkyl groups on hydrocarbon anion radicals and the approaching cation have been known to alter ESR coupling constants for some time now.³³ Studies in tetrahydrofuran (THF) have shown that placement of the methyl groups on the 1,5 positions of the naphthalene anion radical prevents the Na^+ cation from approaching the anion as closely as it does the unsubstituted anion radical, as evidenced by the smaller A_{Na} value for the substituted ion pair.³⁴ In contrast to this, a larger sodium hyperfine splitting is observed for the 2,6-di-*tert*-butylnaphthalene anion radical.^{34,35} This was nicely explained by Goldberg and Bolton,³⁴ wherein they generated a complete spin density contour map of the anion and showed how the *tert*-butyl groups force the Na^+ ions to the positions of higher spin density.

Although there are several studies concerning steric effects upon ion association, this is the first study to our

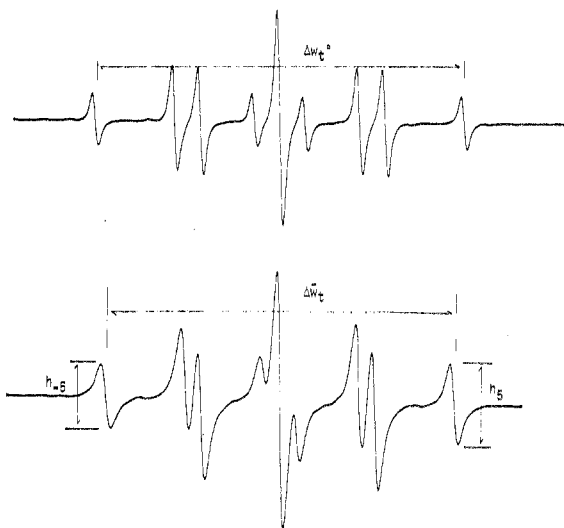


Figure 7. ESR spectra of the ninhydrin anion radical in HMPA. The upper spectrum was taken without the addition of salt and $\Delta\omega_5^0 = 4.390$ G. The lower spectrum was taken after the addition of 0.067 M KClO_4 and $\Delta\omega_5 = 4.134$ G. The small capillary tube containing the cyclooctatetraene anion radical was removed from the EPR cavity area to record these spectra.

knowledge of the steric effects upon the kinetic and/or thermodynamic parameters controlling ion pair dissociation to form the free solvated ions.

Experimental Section

The ESR line positions were determined by sealing the anion radical solutions into ESR tubes that also contained a small capillary tube that contained a sample of the anion radical of cyclooctatetraene (COT) in HMPA. The ninhydrin anion radical ESR spectra could, thus, be obtained simultaneously with that for COT^- or by itself by inverting the sample tube (Figures 3 and 7). The ninhydrin anion radical ESR relative line positions were taken from the distance (d_5) from the central line of the COT anion radical to the high-field line of the ninhydrin anion radical (Figure 7). For an anion radical solution that does not contain any added salt this distance is $d_5^0 = 2.364$ G. The change in the position of the high-field line relative to that for the free ion ($\omega_5^0 - \bar{\omega}_5$) and relative to that for the ion pair ($\omega_5' - \bar{\omega}_5$) are given by eq 11 and 12, where $|\gamma_e|$ is the gyro-

$$(\omega_5^0 - \bar{\omega}_5) = (d_5^0 - d_5) |\gamma_e| \quad (11)$$

$$(\omega_5' - \bar{\omega}_5) = (d_5 - d_5') |\gamma_e| \quad (12)$$

magnetic ratio for an electron (1.7608×10^7 rad/s). X_5 can now be taken directly from eq 5 and is equal to

$$X_5 = P_f(\omega_5^0 - \bar{\omega}_5)^2 + P_c(\omega_5' - \bar{\omega}_5)^2 \quad (13)$$

Likewise, X_{-5} was determined from the change in the position of the low-field line relative to that for the free ion ($\omega_{-5}^0 - \bar{\omega}_{-5}$) and relative to that for the ion pair ($\omega_{-5}' - \bar{\omega}_{-5}$). The value for d_{-5}^0 is $\Delta\omega_{-5}^0 + d_5^0 = 6.754$ G.

The ESR spectra were run on a Varian E-4 or Varian E-9 ESR spectrometer. All of the inorganic salts were purchased from Alfa Inorganics and were stored in a vacuum oven for at least 48 h at 100 °C prior to use. The HMPA was distilled under vacuum from calcium hydride

and stored over molecular sieves. Portions of this HMPA were then distilled directly into the evacuated apparatus for anion radical generation from a small piece of potassium metal. The anion radicals were generated in the apparatus previously described.¹⁷

A kinetic study on the ninhydrin $^-$ -(Bu) $_4$ N $^+$ system could not be carried out due to the fact that the line positions did not change sufficiently upon ion pair formation.

The plots shown in Figures 1 and 2 are examples taken from a set of experiments. Several such plots were generated for each of the systems studied; and since the error in K_{id} propagated from the errors in the intercept and slope of a single plot is smaller than the standard deviation in the K_{id} 's taken from a number of such plots, it is this latter standard deviation that is reported as the error in the text.

References and Notes

- (1) Bjerrum, N. K. *Dan. Vidensk. Selsk. Math., Fys. Medd.* **1926**, *7*, 3.
- (2) Fuoss, R. M. *J. Am. Chem. Soc.* **1958**, *80*, 5059.
- (3) Diggle, R. M.; Boggsanyi, D. *J. Phys. Chem.* **1974**, *78*, 1018.
- (4) Levin, G.; Jagur-Grodzinski, J.; Szwarc, M. *J. Am. Chem. Soc.* **1970**, *92*, 2268.
- (5) Normant, H. *Angew. Chem., Int. Ed. Engl.* **1967**, *6*, 1046.
- (6) Mayer, U. *Coord. Chem. Rev.* **1976**, *21*, 159.
- (7) Gutman, V. *Fortschr. Chem. Forsch.* **1972**, *27*, 59.
- (8) Birtles, R. H.; Hampson, G. C. *J. Chem. Soc.* **1937**, 10.
- (9) Webster, B. M. "Progress in Stereochemistry"; Klyne, W.; de la Mare, P. B. D., Ed.; Academic Press: New York, 1958.
- (10) Geske, D. H.; Ragle, J. L. *J. Am. Chem. Soc.* **1961**, *83*, 3532.
- (11) (a) Meisel, D.; Neta, P. *J. Am. Chem. Soc.* **1975**, *97*, 5198. (b) Neta, P.; Meisel, D. *J. Phys. Chem.* **1976**, *80*, 519.
- (12) Stevenson, G. R.; Fraticelli, Y.; Concepcion, R.; *J. Am. Chem. Soc.* **1976**, *98*, 3410.
- (13) (a) Stevenson, G. R.; Echegoyen, L. *J. Phys. Chem.* **1973**, *77*, 2339. (b) Stevenson, G. R.; Alegria, A. E.; Block, A. R. *J. Am. Chem. Soc.* **1975**, *97*, 4859.
- (14) Stevenson, G. R.; Echegoyen, L.; Hidalgo, H. *J. Phys. Chem.* **1975**, *79*, 152.
- (15) Adam, F. C.; Weissman, S. I. *J. Am. Chem. Soc.* **1958**, *80*, 1518.
- (16) Atherton, N. M.; Weissman, S. I. *J. Am. Chem. Soc.* **1961**, *83*, 1330.
- (17) Stevenson, G. R.; Alegria, A. E. *J. Phys. Chem.* **1976**, *80*, 69.
- (18) Alegria, A. E.; Fontanez, F.; Stevenson, G. R. *J. Phys. Chem.* **1976**, *80*, 1113.
- (19) (a) Stevenson, G. R.; Martir, W. *J. Phys. Chem.* **1976**, *82*, 1171. (b) Martir, W.; Alegria, A. E.; Stevenson, G. R. *J. Am. Chem. Soc.* **1976**, *98*, 7955.
- (20) Fraenkel, G. K. *J. Phys. Chem.* **1967**, *71*, 139.
- (21) (a) Ocasio, I.; Sullivan, P. D. *J. Am. Chem. Soc.* **1979**, *101*, 295. (b) Jones, M. T.; Ahmed, R.; Kastrop, R.; Rapini, V. *J. Phys. Chem.* **1979**, *83*, 1327. (c) Barzaghi, M.; Cremaschi, P.; Gamba, A.; Oliva, C.; Simonetta, M. *J. Am. Chem. Soc.* **1978**, *100*, 3132.
- (22) Stevenson, G. R.; Echegoyen, L. *J. Phys. Chem.* **1973**, *77*, 2339.
- (23) Stevenson, G. R.; Valentin, J.; Williams, E.; Caldwell, G.; Alegria, A. E. *J. Am. Chem. Soc.* **1979**, *101*, 515.
- (24) Stevenson, G. R.; Echegoyen, L. *J. Phys. Chem.* **1973**, *77*, 2339.
- (25) Stevenson, G. R.; Alegria, A. E. *J. Phys. Chem.* **1973**, *77*, 3100.
- (26) Alegria, A. R.; Concepcion, R.; Stevenson, G. R. *J. Phys. Chem.* **1975**, *79*, 361.
- (27) Stevenson, G. R.; Echegoyen, L.; Lizardi, L. R. *J. Phys. Chem.* **1972**, *76*, 1439.
- (28) Stevenson, G. R.; Alegria, A. E. *J. Phys. Chem.* **1975**, *79*, 1042.
- (29) Chauhan, B. J.; Fawcett, W. R.; Lasia, A. *J. Phys. Chem.* **1977**, *81*, 1476.
- (30) (a) Hazelrigg, M. J.; Bard, A. J. *J. Electrochem. Soc.* **1975**, 122. (b) Lasia, A.; Kalinowski, M. K. *J. Electroanal. Chem.* **1972**, *36*, 511.
- (31) (a) Ryan, M. D.; Evans, D. H. *J. Electrochem. Soc.* **1974**, *121*, 881. (b) Krygowski, T. M.; Lisztajn, M.; Galus, Z. *J. Electroanal. Chem.* **1973**, *42*, 261.
- (32) Tushima, S.; Itaya, K. *Bull. Chem. Soc. Jpn.* **1976**, *49*, 957.
- (33) Crowley, A.; Hirota, N.; Krellick, R. *J. Chem. Phys.* **1967**, *46*, 4815.
- (34) Goldberg, I. B.; Bolton, J. R. *J. Phys. Chem.* **1970**, *74*, 1965.
- (35) Goldberg, I. B.; Crowe, H. H. *J. Phys. Chem.* **1976**, *80*, 2603.